CONF-830451--18

CONF-830451--18

DE83 014346

The Effect of Composition and Radiation on the Hertzian Indentation Behavior of Nuclear Waste Glasses

Hj. Matzke,[a] L. Kahl,[b] J. L. Routbort,[a,c]* and J. Saidl[b]

[a]Commission of the European Communities
Joint Research Centre
Karlsruhe Establishment
European Institute for Transuranium Elements
Postfach 2266
D-7500 Karlsruhe
Federal Republic of Germany

[b]Kernforschungszentrum Karlsruhe
Institut fur Nukleare Entsorgung
Postfach 3640
D-7500 Karlsruhe
Federal Republic of Germany

[c]Materials Science and Technology Division
Argonne National Laboratory, Argonne, IL 60439, U.S.A.

*Work partially supported by the U.S. Department of Energy.

The Effect of Composition and Radiation on the Hertzian Indentation Behavior of Nuclear-Waste Glasses

Hj. Matzke,[a] L. Kahl,[b] J. L. Routbort,[a,c]* and J. Saidl[b]

[a]Commission of the European Communities
Joint Research Centre
Karlsruhe Establishment
European Institute for Transuranium Elements
Postfach 2266
D-7500 Karlsruhe
Federal Republic of Germany

[b]Kernforschungszentrum Karlsruhe
Institut fur Nukleare Entsorgung
Postfach 3640
D-7500 Karlsruhe
Federal Republic of Germany

[c]Materials Science and Technology Division
Argonne National Laboratory, Argonne, IL 60439, U.S.A.

Abstract

The Hertzian indentation technique has been used to determine the fracture toughness, K_{Ic} of two borosilicate glasses developed to contain high-level nuclear waste. For the product VG 98/12, adding selected groups of fission products leaves K_{Ic} unchanged, but addition of Pb lowers K_{Ic} by ~ 20%. Radiation with 77 MeV α-particles to a dose of ~ 10^{15} α/cm^2 increases K_{Ic} by ~ 75%. For the product SM 58 LW 11, the fracture toughness was measured on pieces taken from different parts of a large cylinder to investigate the effects of segregation phenomena and of partial crystallization and formation of small cristobalite inclusions which decrease K_{Ic} by ~ 25%.

---

*Work partially supported by the U.S. Department of Energy.

I. Introduction

The Hertzian indentation technique in which a spherical indentor is pressed with a measured load onto the polished surface of a specimen at a given rate until a ring crack forms has been shown to yield valuable information concerning the fracture properties of small samples for which no other procedures are practical. For example, the technique has been used to determine the effect of radiation damage on the fracture toughness of a borosilicate glass,[1] a celsian glass-ceramic,[2] and a nuclear fuel, ThO_2.[3] It has also been utilized successfully to determine the surface fracture energy and the fracture toughness of some nuclear fuels for which large samples required to measure these properties using more conventional techniques are not available, i.e., $(U,Pu)N$[4] and $(U,Pu)C$.[5]

The fracture properties of a nuclear waste containing material have received limited attention, in spite of the fact that deleterious effects could occur if the fracture toughness were severely lowered during the storage period. This could lead, for example, to premature fracture resulting in an enhanced leaching rate. Indeed, the fracture toughness can be affected by radiation damage[1] and by compositional changes,[2] the latter occurring, for example, as the result of segregation due to thermal gradients or radiation.

Therefore, in this paper, the effects of radiation and compositional changes on the fracture toughness as determined from the Hertzian indentation technique of a borosilicate glass without nuclear wastes (VG 98/12) and with simulated fission products (GP 98/12) will be reviewed. The

results will be compared to those obtained on another glass with waste products SM 58 LW 11 which because of segregation during cooling from the melt contained a gradient in composition, primarily a crystobalite phase.

II. Experimental Details

Materials

Two types of borosilicate glasses designed to contain high level nuclear waste (HLW) were investigated. The first product (Versuchsglas VG 98/12), was produced at the INE, KFK Karlsruhe.[6] Laboratory scale samples were employed which were fabricated by melting well-mixed powders in crucibles at 1200°C, 2h and casting into cylinders of about 25 mm dia. and 20-40 mm length. These samples were cooled from 600 to 100°C over a period of 17h. The second material designated as SM 58 LW 11 was used as pieces obtained from a large scale cast cylinder which cooled by natural convection and showed liquid/liquid segregation phenomena followed by crystallization of cristobalite (cooling time 72 h).

The compositions of the glasses are shown in Table 1. Both the base glass VG 98/12 without simulated fission products and the versions containing either 15 wt.% simulated fission product oxides (for GP 98/12) or 11 wt.% low enriched waste concentrate, LEWC of the Eurochemic reprocessing plant Mol (Belgium) were used.

The main difference between the two products is the relatively high content of Li_2O in SM 58 FR replacing part of the Na_2O of the VG 98/12. The waste composition is also different due to the specific properties of

the Eurochemic waste. The latter contains Na_2O, F and SO_3 and less fission products than the nominal HLW used for GP 98/12. The most abundant fission product is Zr, added in the form of ZrO_2. A specific feature of the product SM 58 LW 11 is its liquid-liquid demixing at temperatures below 900°C giving rise to one crystalline form of SiO_2, cristobalite, on further cooling. Since the experiments are performed at room temperature, cristobalite exists in its low temperature form. During the transition from the high temperature to the low temperature form at about 150°C, a volume decrease of about 15% occurs. Further crystalline phases connected to cristobalite formation which were present were small quantities of rutile (TiO_2) and perovskite ($CaTiO_3$), and very minute quantities of Li_2TiSiO_5 and unsoluble precipitates of RuO_2.

This liquid-liquid demixing and the subsequent crystallization lead to a segregation causing streaks in the final product. Figure 1 shows a section of a cylinder. The streaks are clearly visible. Figure 2 shows in more detail that the brighter colors in the streaks are due to formation of cristobalite crystals up to 100 µm in size. Because of the higher density of cristobalite, stresses originate and the matrix around the cristobalite is under tension. For the experiments, the homogeneous product, the most cristobalite-rich zones and an intermediate region were selected for measurements. These were designated homogeneous, strong streaks and slight streaks, respectively.

Technique

The Hertzian crack technique has been described in detail before.[7,8] The tensile elastic stress field which results from indenting the glass surface with a spherical ball produces ring cracks which are detected by acoustic emission and by optical microscopy. The experiments were performed at room temperature in a glovebox containing a dry (0.01% H_2O) nitrogen atmosphere.

For irradiations, the specimens were either exposed to 77 MeV α-particles produced by the cyclotron of the KFK, or bombarded with mass-separated ions in the Institut für Angewandte Kernphysik (IAK, KFK). Rutherford backscattering (RBS) spectra with 2.8 MeV He-ions were performed at the Van de Graaff accelerator of the IAK.

To evaluate fracture surface energy, γ_f, and fracture toughness, K_{Ic}, the critical load to fracture, P_c, and the crack radius, r, must be known. P_c was determined from plots of fracture probability versus load as the load that leads to a 50% probability of fracture. Circular ring cracks were formed whenever P_c was approached or surpassed, similar to those shown before for other materials (e.g., 4,7,8). Their radii, r, were measured in the optical microscope. From the ratio r/a, with a = calculated contact area between indentor and sample (see 7,8), the crack extension function $(a/c")\ [\phi"]^{-2}$ can be obtained from Refs. 7 and 8. The fracture toughness is then calculated from the equation

$$K_{Ic} = \left[\frac{2P_c E}{\beta k R (a/c")\,[\phi"]^{-2}}\right]^{1/2}$$

where $\beta = 8\pi^3/27 \sim 9.18$ is a numerical constant and k is a measure of the elastic mismatch between indentor and specimens. To calculate $k = (9/16)\,[(1-\nu^2) + (1-\nu'^2)\,(E/E')]$, the elastic moduli E and E' and the Poisson ratios ν and ν' of sample and the steel indentor (primed symbols; with $E' = 210$ GPa and $\nu' = 0.29$) must be known. For VG 98/12, a measured value of 72.1 GPa was used, for SM 58 LW 11, a measured value of 88.2 GPa was taken. The measured ν for SM 58 LW 11 was 0.229 and $\nu = 0.2$ for VG 98/12 was assumed.

III. Results

Figure 3 shows the probability of formation of a Hertzian ring crack as a function of applied load P, obtained on the base glass (VG 98/12) for one indentor size (R = 3 mm). The critical load deduced is shown in Table 2, where also the composition of glasses obtained by adding selective groups of additives to the base glass VG 98/12 are shown. These variations are called ABRA 2 to ABRA 6 and contain either corrosion products, rare earths, alkali metals or lead. All glasses had polished surfaces and the indentor radius R = 3 mm was kept constant. The corrosion products were added because they occur in HLW by dissolution of steel, the rare earth and the alkali metals represent typical groups of fission products with high abundance, and PbO was added because it is sometimes used to simulate actinides and because bombardment with Pb-ions is often used to introduce radiation damage. In reality Pb does not occur in solidified waste. The critical loads deduced from Fig. 3 are used to calculate fracture toughness

values which are summarized in Table 2. Note, that only one indentor radius was used for the ABRA-series of glasses. Parallel work[2] with VG 98/12 had shown that a linear relation between P_c and R is obtained as predicted theoretically. Therefore, error limits are given for the K_{Ic}-value of the base glass VG 98/12 but not for the glasses of the ABRA series.

Results for the three types of the second glass product, SM 58 LW 11, without streaks, with slight streaks or with strong streaks are shown in Figs. 4-6. Figure 4 shows the probability for fracture for three different steel identor radii for the homogeneous glass product, whereas Fig. 5 gives the comparison for the product which underwent demixing as shown in Figs. 1 and 2. The resultant plot of critical load versus indentor radius is shown in Fig. 6. Straight lines passing through the origin are indicated up to R = 3 mm whereas the slope changes for bigger indentors. Experiments on regions of this glass containing various flaw size distributions indicate that the deviation from a straight line intersecting the origin (Auerbach's Law) is due to flaw statistics becoming important for the larger indentors. Theory[7] predicts that the size of the flaws necessary to initiate crack formation increases with the indentor radius. If insufficient flaws of appropriate size are available, crack formation depends on flaw statistics thus giving rise to a smaller slope in a plot of fracture probability versus applied load and thus to a higher apparent P_c. For the calculation of K_{Ic}, only the results for indentors with R = 1.5 and R = 3 mm were used. The values of K_{Ic} obtained were 1.16, 1.02, and 0.91 $MNm^{-3/2}$, for

the homogeneous material, the material with slight streaks and the material with strong streaks, respectively. The relevant results are summarized in Table 3.

The effect of radiation, studied on samples bombarded with α-particles in the cyclotron or with Pb ions in a mass-separating accelerator, showed an important toughening of the glass VG 98/12. For bombardment with 200 μAs of 77 MeV He-particles, K_{Ic} increased from 1.8 to 3.1 $MNm^{-3/2}$. Bombardment with lead ions of 300 keV energy (corresponding to a range of ~ 0.2 μm) reduced K_{Ic} to ~ 1.5 $MNm^{-3/2}$ but this value was still higher than that of the glass ABRA 6 containing chemically added lead.

Rutherford backscattering of the base glass, as shown in Fig. 7, or of the fission product (FP) containing glass as shown in Fig. 8, proved that the nominal composition corresponded well with the measured one. As shown in Table 4, the different elements contained in the glass give rise to different contributions in the RBS spectrum: the higher the atomic number, the larger the relative contribution. Also, the higher the mass, the lower the energy loss in scattering. The calculated spectra, shown as thin lines, are based on Table 4 and show good agreement with the measured spectrum for the base glass whereas agreement is achieved for the FP containing glass GP 98/12 only whenever an adjustment is made for the fission products as is shown by the thin full line and the thin dashed line in the lower part of Fig. 8. Agreement between calculation and experimental spectrum is obtained, if the reasonable assumption is made that most of the rare metals, Ru, Rh and Pd are not detected because they are precipitated in

inclusions and that part of Te and Cs, as volatile elements, were lost during fabrication.

Figures 7 and 8 also contain spectra from leached glasses. Leaching was performed in autoclaves in water at 200°C which gives rise to a pressure of ~ 15 bar. The purpose of these experiments was not to study the kinetics of growth of leaching layers which is known to be complex but rather to determine the composition of these layers. Later work will study the effect of such layers on fracture properties.

As shown in Fig. 7, surface peaks appear at the masses of Ti and Ca indicating layer formation with enrichment in Ti and Ca by about a factor of 3 and a thickness of about 0.5 μm, in good agreement with a determination based on the interference colors of the layer formed. Some depletion in Na for about the same depth is apparent while Mg becomes enriched. The fission product containing glass, leached for the same time and shown in the middle of Fig. 8, shows a Ti peak of similar properties as the base glass whereas any Ca peak is much less pronounced. However, both the light and the heavy fission products show one peak each, the one for the heavy fission products being more pronounced. The peak at channel 500 is due to uranium. The enrichment is again by about a factor of 3. At longer leaching time, the peaks become wider with a width of about 0.8 μm. Note in this respect that a depth of 1 μm as indicated in Fig. 8 corresponds to

about 260 keV* or 51 channels, based on energy loss data reported previously.[9] At the longer annealing times, the enrichment in uranium is still visible but amounts to only a factor of 2. The heavy fission product and the light fission products give rise to peaks that overlap, the enrichment in heavy fission products is again a factor of ~ 3 whereas the light fission products are enriched by about a factor of 5. Peaks for Ti and, more pronounced for Ca, are also indicated. The Ca peak is wider than the Ti peak pointing to a Ca-rich subsurface layer. Depletion in Na is pronounced and extends to at least 1 μm.

Preliminary studies on leaching experiments with ion bombarded glasses (Pb and Xe, 300 keV, doses of between $5x10^{12}$ and $5x10^{15}$ ions/cm^2) indicated that no dramatic change in layer thickness and at the most very small changes in layer composition occurred.

IV. Discussions and Conclusions

The present experiments confirm previous work[2] that for small indentor radii, good and reliable results can be obtained for waste glasses. Addition of selected groups of elements to the glass VG 98/12 leave K_{Ic} largely unaffected. The only major effect was observed by adding 1.23% PbO (ABRA

---

*This value applies to the position of U or to the 2.6 MeV of energy remaining. The energy loss, dE/dx depends on energy and increases with decreasing energy.[9] For example, 1 μm = 335 keV at 1.5 MeV remaining energy, or at the Si surface position. Note also that dE/dx for the glass and layer may be different which in the final analysis should be taken into account.

6) which decreased K_{Ic} by approximately 20%. However, depending on its valence, lead in a glass can be either an intermediate or a modifier while most of the other additions only modify the glass network. The single bond strength of lead as an intermediate is some 30% lower than that of SiO_2.[10] Hence, the addition of lead might form intermediate bonds resulting in less resistance to fracture because of decreased bond strengths.

The effect of irradiation with He was very pronounced in VG 98/12. An increase of 75% in K_{Ic} was observed, a very positive result indeed for the long time behavior of waste glasses. It should be mentioned that 77 MeV α-particle irradiation results in a uniformly damaged region, at least 500 μm thick. This region is characterized by ionization rather than displacement damage. Therefore, the results may be an example of radiation toughening by ionization damage. Bombardment with 300 keV Pb ions causes a decrease in K_{Ic}, which however was still within the experimental scatter and the resulting K_{Ic} was still larger than that for the Pb-containing glass. Layers formed by leaching could easily be analyzed with Rutherford backscattering. Layer thicknesses and their composition could be measured reliably in a short time. Further work will deal with the influence of such layers on the fracture behavior.

Small amounts of cristobalite decrease K_{Ic} of SM 58 LW 11 by ~ 25% depending on the amount of crystalline phase. Further experiments and detailed microscopy will determine whether this rather unusual decrease in K_{Ic} is due to the tensile stress field surrounding the crystalline phase.

Acknowledgements: The authors are grateful to O. Meyer, G. Linker and K. Kraatz, IAK for performing the lead ion bombardments and the RBS experiments. K. H. Assmus and W. Maier, IAK, conducted the cyclotron irradiations which were financially supported by KFK. Thanks are due to C. Politis, IAK, for measuring the elastic modulus of the VG 98/12 and to D. S. Kupperman, ANL who measured the elastic moduli of SM 58 LW 11. Last but not least the capable experimental assistance of V. Meyritz (TU) is gratefully acknowledged.

REFERENCES

[1]J. L. Routbort, P. Offermann and Hj. Matzke, "Mechanical Stability of a Cm-doped Celsian Glass Ceramic," Proc. 6th Int. Symp. on the Scientific Basis for Radioactive Waste Management-1982, D. G. Brookins, ed., North Holland, New York, in press.

[2]J. L. Routbort and Hj. Matzke, "The Effect of Composition and Radiation on the Fracture of a Nuclear Waste Glass," Mat. Sci. Eng. 58, 229-237 (1983).

[3]Hj. Matzke and J. L. Routbort, "The Effect of He-Irradiation on the Fracture Toughness of ThO_2," J. Nucl. Mat. 116 (1983) in press.

[4]Hj. Matzke and T. Inoue, "Hertzian Indentation of Advanced LMFBR Fuels with Simulated Burn-up," J. Nucl. Mat. 110, 164-172 (1982).

[5]Hj. Matzke, V. Meyritz and J. L. Routbort, "Fracture Surface Energy and Fracture Toughness of (U,Pu)C and (U,Pu)(C,O)," J. Am. Ceram. Soc., 66, 183-188 (1983).

[6]L. Kahl, M. C. Ruiz-Lopez, J. Saidl and Th. Dippel, "Herstellung und Charakterisierung eines Borosilikatglases zur Verfestigung von Hoch Radioaktiven Spaltproduktlösungen (HAW)," Report Kernforschungzentrum Karlsruhe KFK-3251 (1982).

[7]R. Warren, "Measurement of the Fracture Properties of Brittle Solids by Hertzian Indentation," Acta Met. 26, 1759-1769 (1978).

[8]Hj. Matzke, T. Inoue, and R. Warren, "The Surface Energy of UO_2 as Determined by Hertzian Indentation," J. Nucl. Mater. 91, 205-220 (1980).

[9]Hj. Matzke, "Actinide Diffusion in Waste Glasses," p. 311-329 in Thermodynamics of Nuclear Materials 1979, Vol. I, IAEA, Vienna, 1980.

[10]W. D. Kingery, H. K. Bowen, and D. R. Uhlmann, p. 99 in Introduction to Ceramics, Wiley, New York, 2nd ed. (1976).

Figure Captions:

Fig. 1. Section through a full size cylinder of the glass product SM 58 LW 11 showing streak formation during cooling.

Fig. 2. SEM micrograph of streaked area in the SM 58 LW 11 product of Fig. 2 showing crystallization of cristobalite.

Fig. 3. Probability of fracture for Hertzian indentation with spherical steel indentors of radius R = 3 mm on the base glass VG 98/12 and the product ABRA 2 (containing corrosion products), ABRA 3 (containing rare earths), ABRA 4 (containing alkali metals) and ABRA 6 (containing PbO).

Fig. 4. Probability for fracture for Hertzian indentation of the homogeneous product SM 58 LW 11.

Fig. 5. Probability for Hertzian fracture in either homogeneous glass SM 58 LW 11 or in areas with slight streaks or in areas with strong streaks, corresponding to the microstructure of Fig. 2.

Fig. 6. The critical load for crack formation as function of steel indentor radius for the three types of waste glass SM 58 LW 11 in Fig. 5.

Fig. 7. Rutherford backscattering (RBS) spectrum of waste glass VG 98/12 in as-received condition or following leaching for 25 min at 200°C in H_2O. For the as-received condition the calculated spectrum is shown with thin or dashed lines.

Fig. 8. RBS spectrum for the fission product containing waste glass GP 98/12. The lower curve shows the spectrum of the as-received glass together with the calculated spectrum (thin lines). For the discrepancy at about channel 470, see text. The two upper curves show the effect of leaching in H_2O at 200°C for 25 and 90 min.

Table 1: Compositions of the waste glasses (concentrations in mol. % of the oxides)

	VG 98/12	SM 58 FR	GP 98/12	SM 58 LW 11
SiO_2	58.5	62.73	54.9	57.14
B_2O_3	11.0	11.70	10.3	10.65
Al_2O_3	1.6	0.75	1.5	0.69
Li_2O	--	8.29	--	7.55
Na_2O	17.5	4.95	16.4	4.51
MgO	3.2	3.37	3.1	3.07
CaO	4.6	4.52	4.2	4.12
TiO_2	3.6	3.69	3.4	3.36
	100.0	100.00	93.8	91.09
Al_2O_3			--	0.54
BaO			0.30	0.04
CeO_2			0.44	0.06
Cr_2O_3			0.05	0.11
Cs_2O			0.23	0.03
Eu_2O_3			0.09	--
Fe_2O_3			0.10	0.63
Gd_2O_3			0.01	--
La_2O_3			0.11	0.02
Na_2O			--	3.20
Nd_2O_3			0.36	0.05
NiO			0.10	0.34
MnO_2*			0.22	0.42
MoO_2			0.90	0.12
PdO			0.33	0.04
Pr_2O_3			0.10	0.01
Rb_2O			0.05	0.01
Rh_2O_3			0.04	--
RuO_2			0.53	0.07
Sm_2O_3			0.07	--
SrO			0.24	0.03
TeO_2			0.11	0.02
Y_2O_3			0.06	0.01
ZnO			--	0.01
ZrO_2			1.02	0.39
P_2O_5			0.44	<0.01
SO_3			--	0.40
F			--	2.36
UO_2			0.28	--
			100.00	100.00

*for Tc.

GP 98/12 contains 15 wt.% fission product oxides, SM 58 LW 11 contains 11 wt.% low enriched waste concentrate, LEWC, of the Eurochemic Mol (Belgium), both simulated, hence not radioactive.

Table 2: Tabulated results for the base glass VG 98/12 and its modifications.

Material	Designation	Additive (wt.%)	P_c [N] (R = 3 mm)	K^*_{Ic} [$MNm^{-3/2}$]
VG 98/12	Base glass	—	410 ± 20	1.77 ± 0.15
ABRA 2	With corrosion products	0.23 Fe_2O_3 0.10 NiO 0.10 Cr_2O_3	408 ± 20	1.8
ABRA 3	With rare earths	1.08 CeO_2 0.36 Sm_2O_3 0.49 Pr_2O_3 0.06 Eu_2O_3 1.70 Nd_2O_3 0.06 Gd_2O_3	441 ± 30	1.8
ABRA 4	With alkali metals	0.14 Rb_2O 0.91 Cs_2O	476 ± 50	2.0
ABRA 6	With lead	1.31 PbO	270 ± 70	1.4

*A value of E of 72.1 GPa, measured for the base glass, and an assumed value of $\nu = 0.20$ were used for all calculations.

Table 3: Elastic moduli, indentation parameters, fracture surface energy and fracture toughness for SM 58 LW 11

	Material		
	Homogeneous	Slight-streaked	Strong-streaked
E[GPa][a]	88.2 ± 0.4	--	88.3 ± 1.3
ν[a]	0.229 ± 0.001	--	0.226 ± 0.004[b]
P_c/R [N/mm]	72 ± 3	52 ± 2	41 ± 2
r/a	1.21 ± 0.06	1.25 ± 0.06	1.25 ± 0.08
$(a/c")\ [\phi"]^{-2}$	1325 ± 100	1275 ± 100	1275 ± 150
γ_F [Jm^{-2}]	7.5 ± 0.9	5.6 ± 0.7[c]	4.4 ± 0.8
K_{Ic} [$MNm^{-3/2}$]	1.16 ± 0.07	1.02 ± 0.06[c]	0.91 ± 0.08

[a] These values were computed from the longitudinal (25 MHz) and transverse (5 and 10 MHz) sound velocities measured using the echo overlap technique. The measured densities were 2.61 gm/cm^3.

[b] Recent measurements have shown that Poissons ratio is very sensitive to the amount of crystalline phase and can be as low as 0.175.

[c] Calculated using ν = 0.23 and E = 88 GPa.

Table 4: Contribution to Rutherford-backscattering spectra

Component	at.%	Scattering yield, relative to Si	Contribution to RBS-spectrum		Energy remaining following scattering in MeV for	
			Relative to Si	%	2 MeV He	2.8 MeV He
O	59.2	0.33	1.14	25.0	0.74	1.03
Si	17.2	1.00	1.00	21.9	1.14	1.59
Na	10.3	0.62	0.37	8.1	1.00	1.40
B	6.6	0.13	0.05	1.1	0.46	0.63
Ca	1.3	2.04	0.15	3.3	1.34	1.89
Ti	1.1	2.47	0.16	3.5	1.44	2.02
Al	0.9	0.86	0.04	0.9	1.12	1.56
Mg	1.0	0.74	0.05	1.1	1.04	1.45
Xe	ion bom-	14.9	--	--	1.78	2.49
Pb	bardment	34.3	--	--	1.85	2.60
F	0.27	1.15	0.02	0.4	1.20	1.68
Fe,Ni,Cr	0.13	2.94 - 4.00	0.03	0.6	1.48-1.53	2.06-2.14
Mn (for Tc)	0.07	3.18	0.01	0.2	1.50	2.10
Rb,Sr,Y	0.14	6.98 - 7.76	0.06	1.3	1.66-1.68	2.33-2.35
Zr	0.31	8.16	0.15	3.3	1.68	2.36
Mo	0.27	9.0	0.14	3.1	1.70	2.38
Ru,Rh,Pd	0.29	9.8 - 10.8	0.17	3.7	1.71-1.72	2.40-2.41
Te,Cs	0.17	13.8 - 15.4	0.17	3.7	1.77-1.78	2.48-2.49
Ba,La	0.16	16.0 - 16.6	0.15	3.3	1.78	2.50
Ce,Pr,Nd	0.41	17.2 - 18.4	0.42	9.2	1.79	2.50-2.51
Sm,Gd,Eu	0.06	19.6 - 20.9	0.06	1.3	1.80-1.81	2.52-2.53
U	0.09	43.2	0.23	5.0	1.87	2.62

15 wt.% fission product oxides correspond to 2.4 at.% because of their high atomic weights.

The scattering yield is proportional to the square of the atomic number, Z^2. The energy following scattering at the surface increases with the atomic mass, M. Therefore, the contributions of a small amount of heavy atoms, such as Pb, appears as pronounced peak at high energies.

Fig. 1. Section through a full size cylinder of the glass product SM 58 LW 11 showing streak formation during cooling.

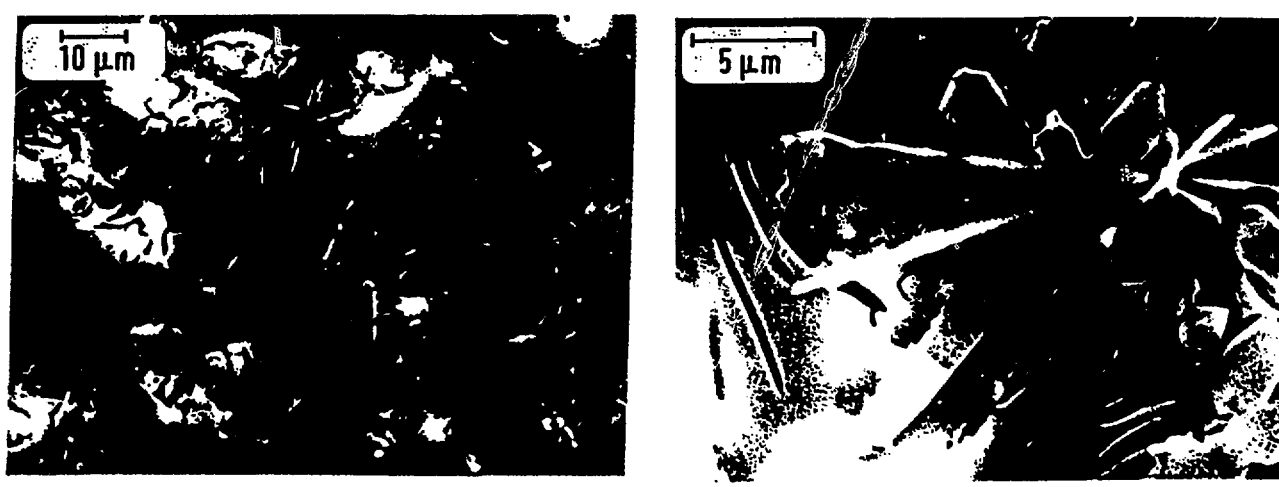

Fig. 2. SEM micrograph of streaked area in the SM 58 LW 11 product of Fig. 2 showing crystallization of cristobalite.

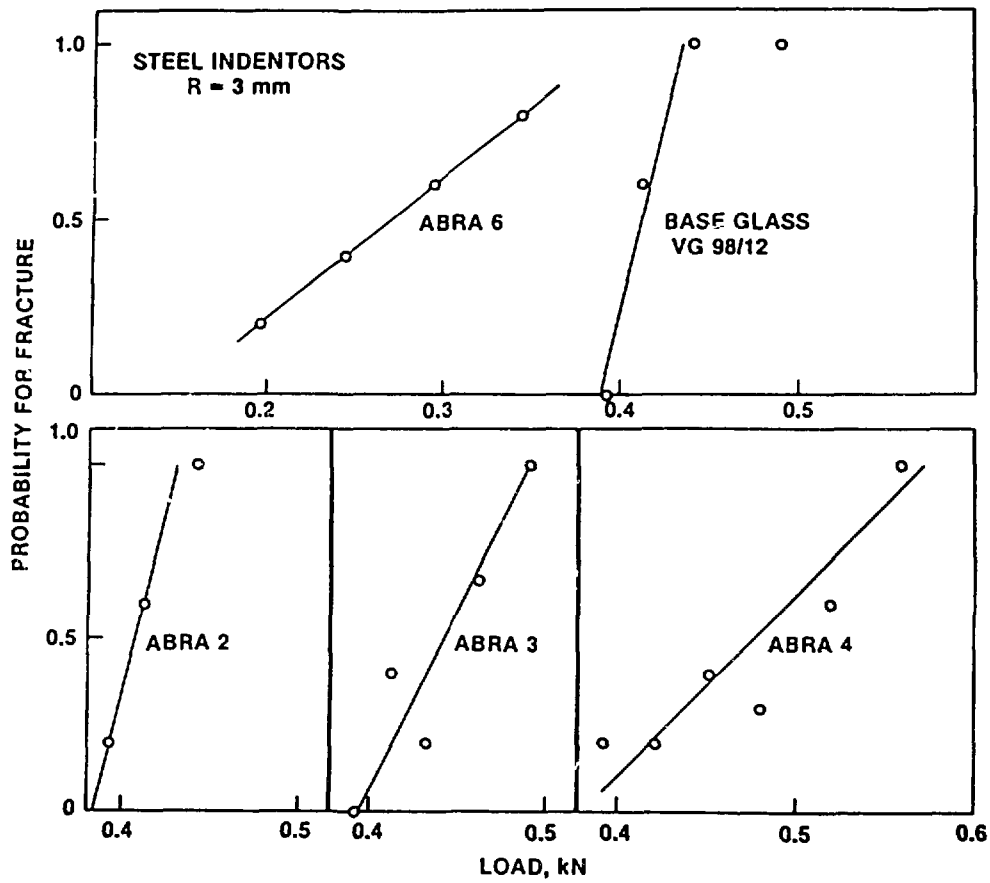

Fig. 3. Probability of fracture for Hertzian indentation with spherical steel indentors of radius R = 3 mm on the base glass VG 98/12 and the product ABRA 2 (containing corrosion products), ABRA 3 (containing rare earths), ABRA 4 (containing alkali metals) and ABRA 6 (containing PbO).

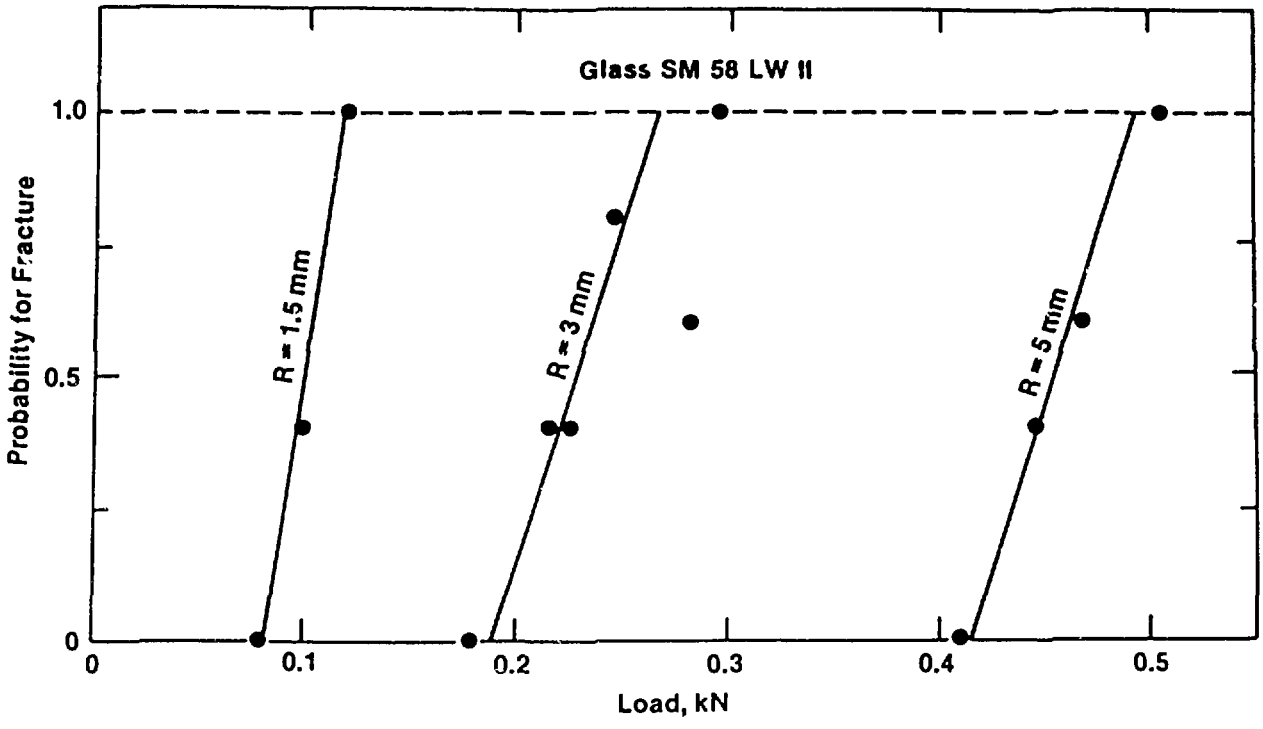

Fig. 4. Probability for fracture for Hertzian indentation of the homogeneous product SM 58 LW 11.

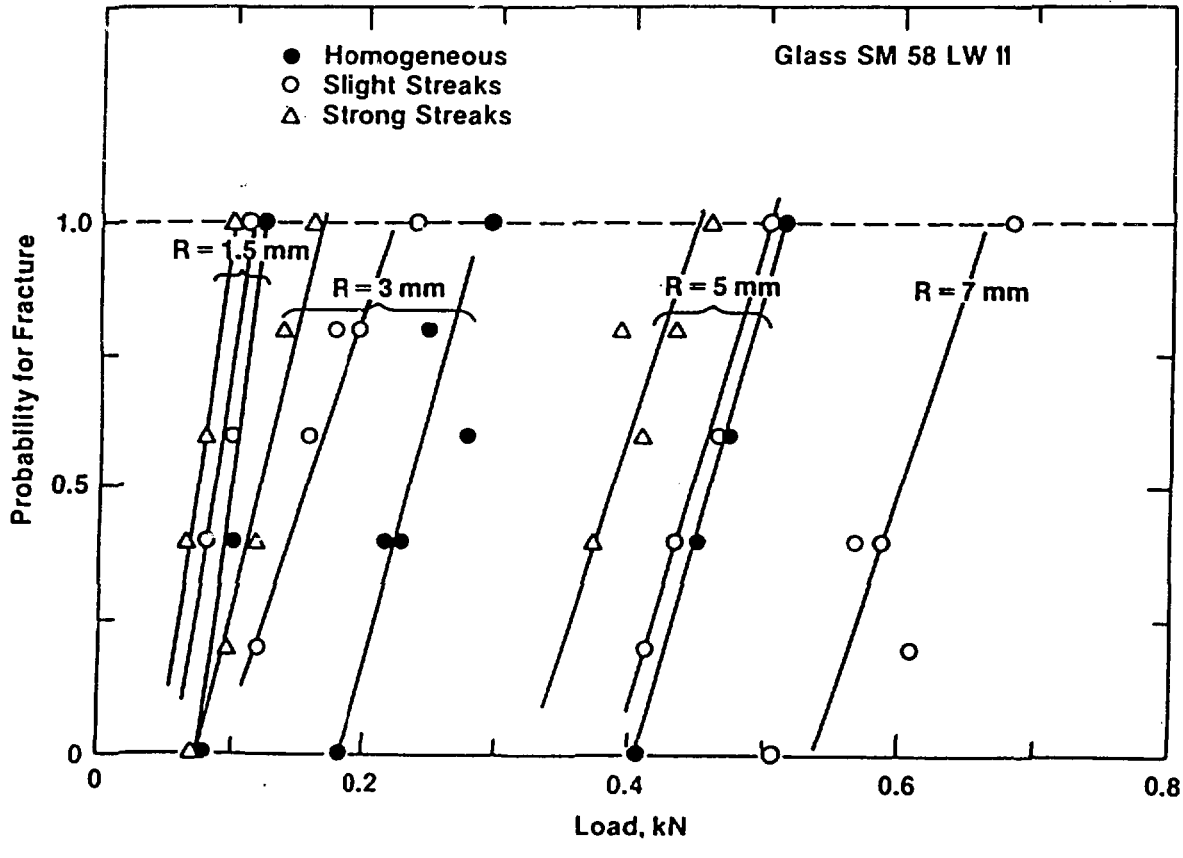

Fig. 5. Probability for Hertzian fracture in either homogeneous glass SM 58 LW 11 or in areas with slight streaks or in areas with strong streaks, corresponding to the microstructure of Fig. 2.

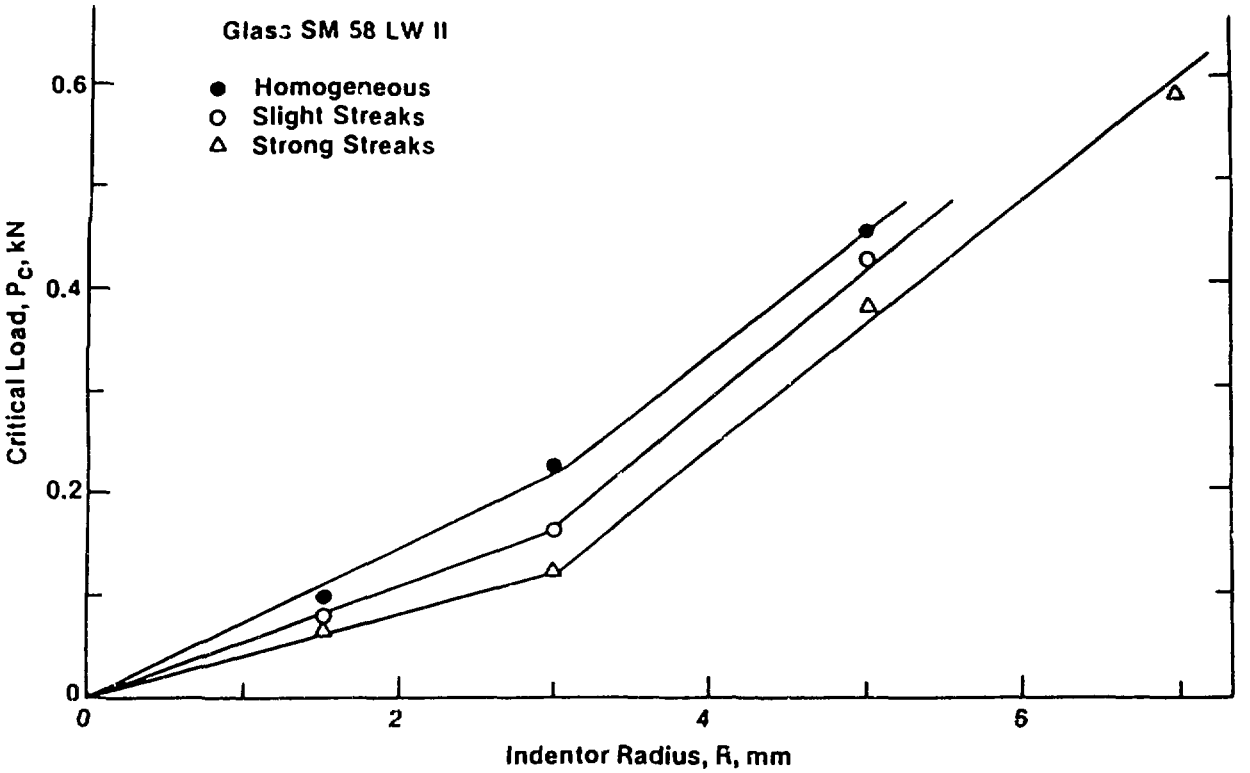

Fig. 6. The critical load for crack formation as function of steel indentor radius for the three types of waste glass SM 58 LW 11 in Fig. 5.

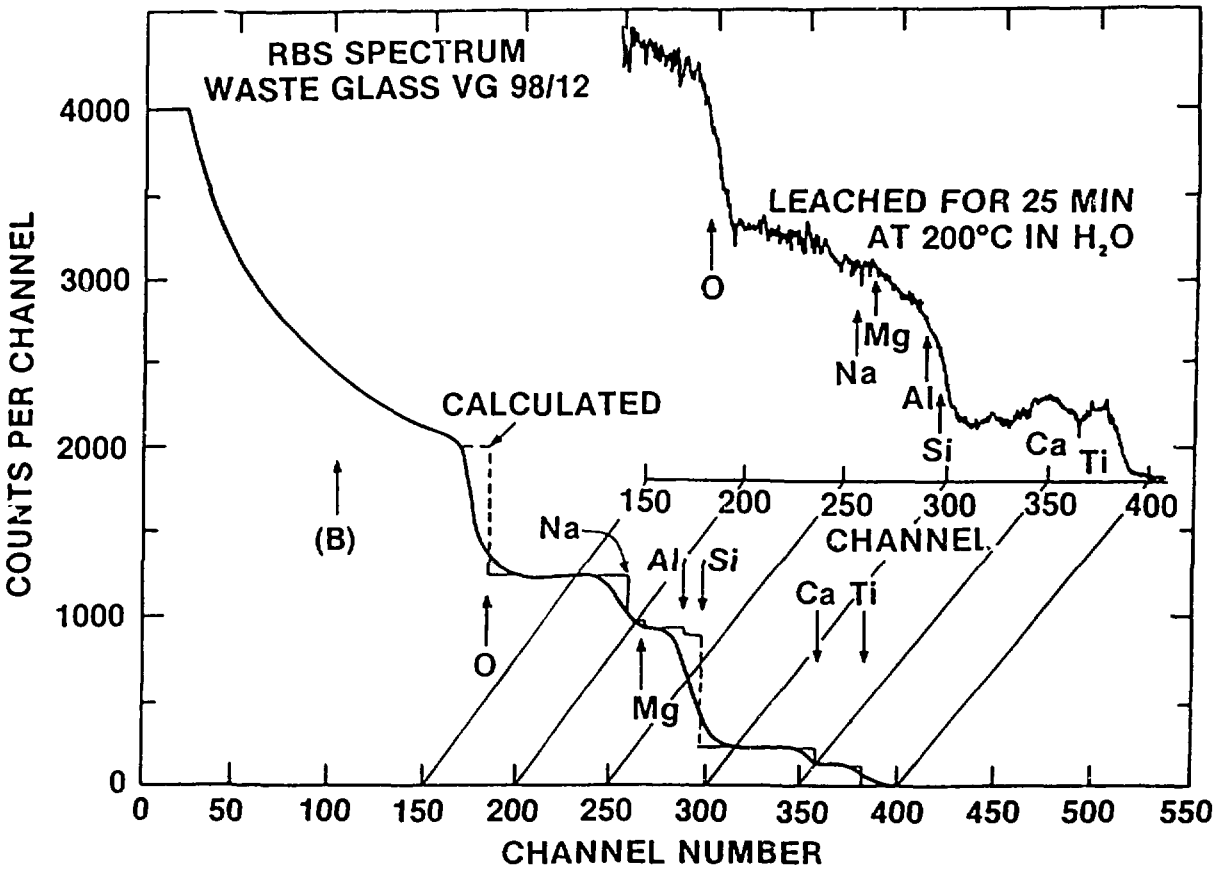

Fig. 7. Rutherford backscattering (RBS) spectrum of waste glass VG 98/12 in as-received condition or following leaching for 25 min at 200°C in H_2O. For the as-received condition the calculated spectrum is shown with thin or dashed lines.

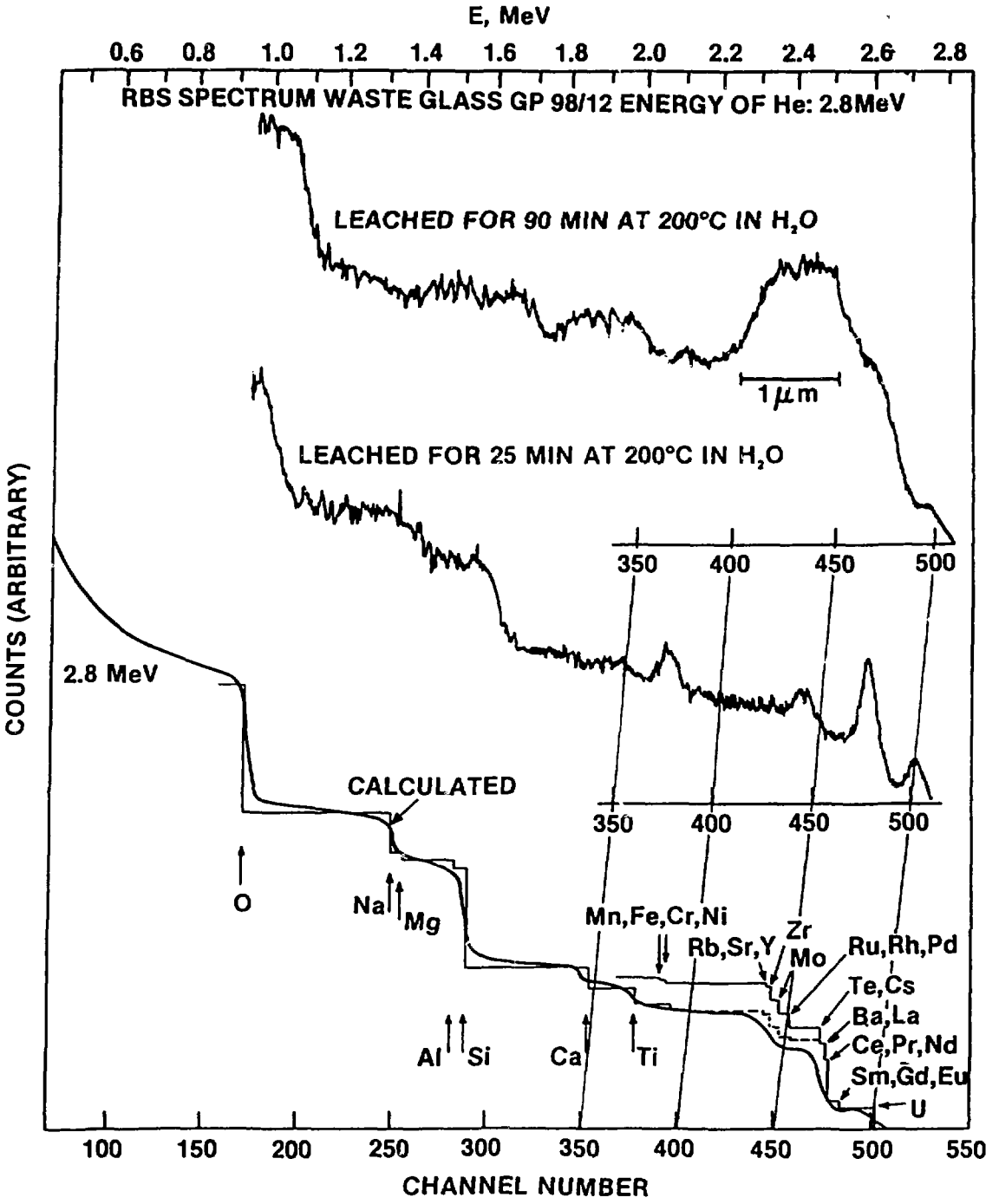

Fig. 8. RBS spectrum for the fission product containing waste glass GP 98/12. The lower curve shows the spectrum of the as-received glass together with the calculated spectrum (thin lines). For the discrepancy at about channel 470, see text. The two upper curves show the effect of leaching in H_2O at 200°C for 25 and 90 min.